AMPLIFICATION OF HIGH ENERGY PICOSECOND OPTICAL PULSES USING SLAB-COUPLED OPTICAL WAVEGUIDE AMPLIFIERS AT 1550NM

A Thesis

Presented to the Faculty of the Graduate School

of Cornell University

In Partial Fulfillment of the Requirements for the Degree of

Master of Science

by

Yen-Wei Tseng

August 2009

ABSTRACT

In recent years there has been a surge of interest in semiconductor optical amplifiers (SOAs) capable of amplifying high energy optical pulses for applications in telecommunication, medical imaging and scientific research. In order for an SOA to be capable of outputting high energy optical pulses, the saturation energy for the particular SOA must be high. The traditional approach to increase the observable device saturation energy of an SOA is to reduce the effect of dynamic gain saturation. However, for high energy picosecond or subpicosecond pulses, peak intensity is significant, and dynamic gain saturation ceases to be the only mechanism responsible for observed device gain saturation. In this thesis, we analyzed the effects of nonlinear absorption within high power SOAs and found that two photon absorption acts as a significant competing mechanism for device gain saturation. Both theory and experimental results are presented in support of this conclusion.

BIOGRAPHICAL SKETCH

David Yen-Wei Tseng was born in 民國 74 年 (1985 C.E.) in Taipei, Taiwan. He went to school in Taiwan until he finished second grade and moved to Orlando, Florida where he attended Aloma Elementary School. After fourth grade, he moved to Gainesville, Florida where he participated in a gifted program focused on math and science at Littlewood Elementary School. He attended Oak Hall School for sixth and seventh grade where he began to have immense interest in science under the guidance of Dr. Lane. He attended eighth and ninth grade in Hingham, Massachusetts where numerous math and science teachers provided him with solid foundations. David moved to Fremont, California to attend Mission San Jose High School where the most valuable classes he took included AP physics, AP chemistry, AP calculus, AP statistics, and photography. In 2003, he attended University of California, Irvine to major in computer engineering only to switch majors to electrical engineering and then finally to double that with computer engineering. During his undergraduate career, he gained research experience through experimenting with optical trapping, noncontact vibrometer, and acousto-optic tunable filters under Professor Henry P. Lee. David joined Professor Farhan Rana's group in the Department of Electrical & Computer Engineering at Cornell University in summer of 2007 where he worked on semiconductor optics and ultrafast optics.

ACKNOWLEDGMENTS

I am grateful to many people who have supported, inspired, guided, and financed me thus far. I will start this with the people who influenced me the most during my two years here at Ithaca. First and foremost, I would like to thank my thesis advisor Professor Farhan Rana, for his guidance, patience and support especially during the time when every module in my experimental setup started to malfunction. His infinite depth and breadth of knowledge in semiconductor optoelectronics is truly inspirational.

I would like to thank Faisal Ahmad, not only as a teammate but also as a friend, in paving the way and making the SCOW projects possible. His ability to recall history will never cease to amaze me. I would also like to thank Misha Kats, who accompanied me in pulling numerous all-nighters in order to meet certain deadlines. That one night before the CLEO deadline, when every part of the experiment went as smooth as it possibly could, was a night to remember. I would like to thank Jahan Dawlaty for his patience as well as his willingness to share his wisdom even at busiest of times. Jahan is a person who could explain the most complicated concept in the simplest of terms. I would like to thank Paul George for his persistence in working with me on the fiber lasers, always suggesting new perspectives in tackling the never ending problem of cw component in the mode lock laser.

I am grateful to my first research advisor, Professor Henry P Lee for exposing me to the field of optics and for giving me so much research opportunities. I would also like to thank Rong Huang, Fares Alhassen, and Patrick Chan for being such supportive lab mates back at UCI.

I want to collectively thank all my friends from Cornell University, UCI, and Mission San Jose High School who took part in these past two years: Jiyeon Hwang,

Mandy Yu, David Li, Allen Lin, Alison Wu, Kuming Chang, Haining Wang, Sunwoo Li, Evan Zhang, Michael Ma, Xiao Wang, Jenny Lin.

Last but not least, I am forever grateful to all members of my family. My mother and father have always supported me in whichever direction I decided to pursue. My sister, Jessica, and brother in law, Will, have given me countless advices. Without them, I would never have accomplished half of what I've accomplished.

TABLE OF CONTENTS

LIST OF FIGURES

LIST OF TABLES

CHAPTER 1

INTRODUCTION

1.1 Motivation

Optical amplifiers are devices that amplify low power continuous-wave or low energy pulsed light. The concept of the amplifier is completely different from a repeater which is a device that detects and then re-emits light. In many cases, optical amplifiers are similar to lasers in that both have a pumped gain medium which establishes population inversion and function by means of stimulated emission. The major difference between an optical amplifier and a laser is the lack of feedback; unlike a laser, since the amplifier is designed to eliminate feedback, an amplifier requires an input in order to output light.

Amplifiers which provide gain (amplification) to optical pulses have found applications in telecommunication, medicine, and many other fields of science and technology. Optical telecommunication is perhaps biggest use for optical amplifiers. The most common form of optical telecommunication today utilizes modulated light from a laser source which travels along fiber-optic cables at nearly the speed of light. In fact, a vast majority of the world's long distance voice and data is carried over optical fiber which enables lower loss and higher bit rate compared to electrical signals.

Losses in single-mode optical fiber (SMF) can accumulate and become significant despite its ultra low loss of just 0.2 dB/km at the communication wavelength of 1550nm. Using repeater technology to detect and then re-emit a signal at regular intervals to boost the signal is both expensive and slow, as the signal needs

to be processed by an electronic circuit. Instead, amplifiers are used to amplify the signal without the conversion to and from electronic signal. The most common type of amplifier used today is an all-fiber amplifier, specifically the erbium-doped fiber amplifier (EDFA). EDFAs are very robust and display phenomenal performance, however they are fairly expensive and contain many components. The simplest of these EDFA require component such as a higher energy wavelength laser diode to pump the erbium-doped fiber, a wavelength division multiplexor, an isolator, and of course the erbium-doped fiber. A key research and engineering challenge is the creation of high power, inexpensive, and compact amplifiers which might replace EDFA technology. This thesis analyzes several challenges in creating high-power semiconductor optical amplifiers (SOA).

1.2 Semiconductors

A semiconductor is a material that displays electric behavior that lies between a conductor and an insulator. Most intrinsic semiconductors at room temperature have low conductivity, and behave very much like insulators. However, one difference that sets apart semiconductor from insulator is that an electron in a semiconductor's valence band requires much less energy to move to the conduction band and become a free carrier. This means that as temperature goes up, a semiconductor becomes electrically conductive faster than an insulator.

Semiconductors's electrical properties can be altered by introducing controlled amount of impurities in the material. The process of introducing these impurities is known as doping. Doping replaces an atom in a semiconductor lattice with a foreign atom that contains one electron more or one electron less than the atoms of the semiconductor itself. This doping process affects the electrical properties of

semiconductor. For example, if a donor atom, a dopant that has one more valence electron than the atom it replaces, is introduced, that extra electron will not be part of the lattice construction. Instead, this electron is free to move around, increasing the conductivity of the semiconductor. A semiconductor that is modified in this way is called n-type because the majority carrier is negatively charged. On the other hand, if the acceptor atom, a dopant that has one less electron than the atom it replaces, is introduced, then a ”hole” (an empty space where an electron should be) is created. It turns out that the hole can move around similar to an electron, which also aids in electrical conductivity. Such a semiconductor is labeled p-doped because the holes act as positive charge carriers. Ignoring the vast majority of complications, today’s favored process for doping is fairly simple: fire the dopant atoms at a piece of semiconductor so that the dopant atoms imbed themselves in the structure, and then heat up the lattice so that the structure re-anneals, wiping out the defects induced by ramming atoms at the lattice. This process is called ion implantation.

Silicon is by far the most common semiconductor in various applications today. Silicon has various properties which make it very favorable compared to other semiconductors. For example, oxide of silicon is very well understood and is very controllable [4] which is important for the creation of reliable and high yield devices, and it retains its semiconductor qualities at fairly high temperatures. Today silicon is the heart of integrated circuit technology and is a part of practically every piece of electronics created. A more recently developed area than that complementary metal-oxide semiconductor (CMOS) technology that is so commonly used in integrated circuits is the field of silicon photonics. Numerous optical components that are in use today are made of silicon. However, these components all share a common trait: they are all passive components. Silicon can be used to guide, modulate, and filter light.

However, an active device, one which provides optical gain, is difficult to make using the indirect bandgap silicon. This means that in order to make active devices such as lasers or optical amplifiers, a different approach must be taken.

The reason active devices are difficult to make from silicon is a material property referred to as indirect bandgap. Understanding this requires a brief understanding of bands in semiconductors which were briefly mentioned earlier in this section. A semiconductor has two energy bands -valence bands, and conduction bands. The valence band is the highest range of energies at various wavevectors where electrons are present when a semiconductor is at absolute zero (at absolute zero, the semiconductor does not conduct at all). The conduction band is the lowest range of energies at various wavevectors that are high enough to allow electrons to flow freely within the material under some external force, for example an applied electric field. The region between the valence and the conduction band is referred to as a band gap.

In a semiconductor, an electron can be promoted from the valence band to the conduction band by absorbing a photon. This transition requires both energy and momentum conservation; and it is precisely this momentum conservation that makes silicon unsuitable for active photonic devices. It turns out that the maximum energy of the valence band of silicon is not at the same k-point as the minimum energy of the conduction band; since a photon has very little momentum, photon absorption is extremely unlikely. In fact, this process can only take if the electron gets an extra momentum ”kick” from a phonon at precisely the right time. This three particle interaction between electron, phonon, and photon is not likely to happen, photon absorption by electron promotion by silicon does not happen often.

For precisely the same reason, an electron in the conduction band cannot easily make the efficient transition to the valence band in silicon and release a photon. As it so happens, this is the requirement for making an active device, so silicon does not fit our purpose.

On the other hand, another class of semiconductors exists for which the maximum of the valence band coincides in k-space with the minimum of the conduction band, creating a direct band gap. These semiconductors are typically compounds of various materials in the III and IV groups of the periodic table, and less commonly in the II-VI groups. Some commonly used direct band gap semiconductors include binary semiconductors such as InP and GaAs, tertiary semiconductors such as InGaAs and GaInP, and quaternary semiconductors such as InGaAsP. These materials can be doped in various ways just as silicon can, and their electrical properties can be further engineered by adding various stresses and strains. A reasonably complete III-V reference chart is displayed in Figure 1.1, showing various III-V materials, their lattice constants, and their band gaps in both wavelength and energy. Note that materials can typically only be grown on top of one another if their lattice constants match, but even with this constraint the III-V semiconductors are very versatile. For example, various InGaAsP, AlGaInP, GaInP, AlAs, and AlInP materials can all be grown on a GaAs substrate; these materials have a band gap range of 1.5~2.5 eV, which allows the creation of devices which exhibit gain at any frequency in the 500nm to 800nm range. For this thesis, we are interested in amplification of light centered at the 1550nm communication channel, so devices that are lattice-matched to InP is the approach taken. At the end of this thesis, we will come back to figure 1.1 again, when discussing future research directions.

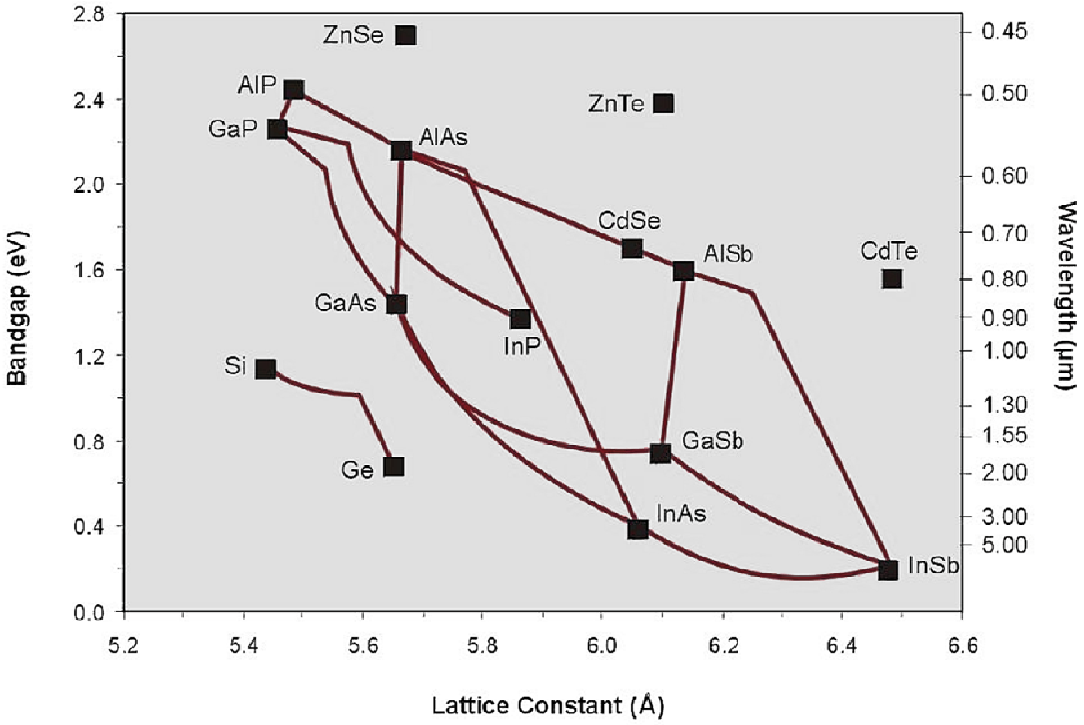

Figure 1.1: Semiconductor Reference Chart

1.3 Semiconductor Optical Amplifiers

Semiconductor Optical Amplifiers are referred to in literature as semiconductor laser amplifiers (SLAs). Despite the fundamentally complex dynamics inside an SOA, the basic concept is fairly easy to understand.

The most basic SOA closely resembles a PIN diode; where the intrinsic region is sandwiched between the p-doped and n-doped semiconductor which is displayed in Figure 1.2. The upper part is a region of p-type semiconductor in which holes serve as the carriers, the lower part is an n-type region in which electrons serve as carriers, and there's an undoped section in the middle. Metal contacts at the top and bottom of the structure finish off our basic SOA.

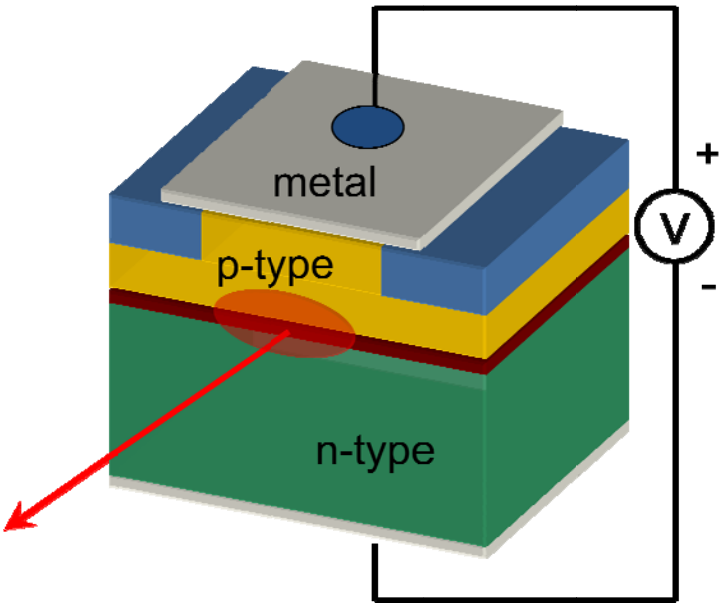

Figure 1.2: Basic SOA Structure

The intrinsic section of the structure possesses a lower band gap than both n-type and the p-type regions, which gives this device two important properties. The first is that the lower band gap provides the carriers a lower potential to gather in this region, which increases probability for the electrons and holes to recombine and, if the semiconductor has a direct band gap as in the case of III-V semiconductors, emit a photon. When the device is forward biased hard enough, sufficient current is passed through the device in the direction of p-type to n-type semiconductor, the carrier density in the intrinsic region increases, and the region begins to display gain by stimulated emission.

The second property, which applies to all semiconductors, is that the band gap is inversely proportional to its refractive index. This relation means that the refractive index of the intrinsic region, with its lower band gap, is higher than the refractive index of the n and p-type regions; such a structure confines the guides light along the

length of the device in much the same way as an optical fiber guides light. This structure is typically referred to as a waveguide.

The final component of SOA is the anti-reflective coating on the facets. Spontaneous emission of coherent light, also known as lasing, can happen if feedback, light reflecting back into the device, within the cavity is not inhibited. Lasing is not a desirable behavior for an amplifier, whose ideal operation is to amplify the input signal and nothing else. Reflection off the facets of the device which are formed when the device is cleaved along crystal planes is the primary cause of feedback in an SOA. This cleaving procedure is necessary not only to remove an individual device from the rest of the wafer but also to provide an interface for maximum coupling efficiency into and out of the device. Cleaving along a crystal plane creates facets that are uniform down to the atomic level and are naturally about 30% reflective. This reflectance is eliminated by application of an anti-reflective (AR) coating on the facets, which reduces the reflectivity. The specific AR coating procedure will be discussed in the Device Geometry section.

It is important to note that without the AR coatings, a way to reduce or eliminate feedback, the SOAs are no different than continuous wave (CW) semiconductor lasers. In fact, by changing the facet coatings from anti-reflection to high-reflection (HR), an amplifier can be made into a CW laser, and vice versa. Due to this close relationship between CW laser and amplifier, one could use the measured performance of an amplifier to make statements about the physics in a semiconductor laser, and vice versa. This is precisely what we do in later sections of this thesis.

Actual fabricated SOAs are typically only a little more complex than the simplified description provided in this section. In an actual SOA the gain section is

composed of, and surrounded by, a structure that is more than a simple layer of intrinsic material. For example, a thin 10nm layer confines electrons and holes much more than a thicker 100nm layer, yielding very distinct energy levels. Such a confined structure is a called a quantum well. Other possibilities for the gain medium includes using multiple quantum wells, as well as quantum wires, quantum dots, quantum dashes, among others, all of which have very different properties which can be exploited to obtain desired behavior. An essential modification include a separate confinement heterostructure (SCH), which is a layer that surrounds the gain section and serves to confine the optical mode. Because the n and p-type regions are optically very lossy and any mode overlap with these doped regions degrades device performance, the SCH is necessary to confine the optical mode away from these doped regions.

Figure 1.3 shows a diagram of the bandgap and refractive index of a typical SOA. The device shown uses quantum well for the gain region and a separate confinement heterostructure to confine the optical mode.

While SOAs have been around for quite some time, they have found limited application for pulse amplification and have been overshadowed by fiber amplifiers both in research and industrial uses partially due to the inferior performance. For example, modern EDFAs show large amounts of gain at 1550nm with output energies measured in hundreds of microjoules. Conventional SOAs, on the other hand, seldom break 10 picojoules – seven orders of magnitude lower than what EDFAs can output[5].

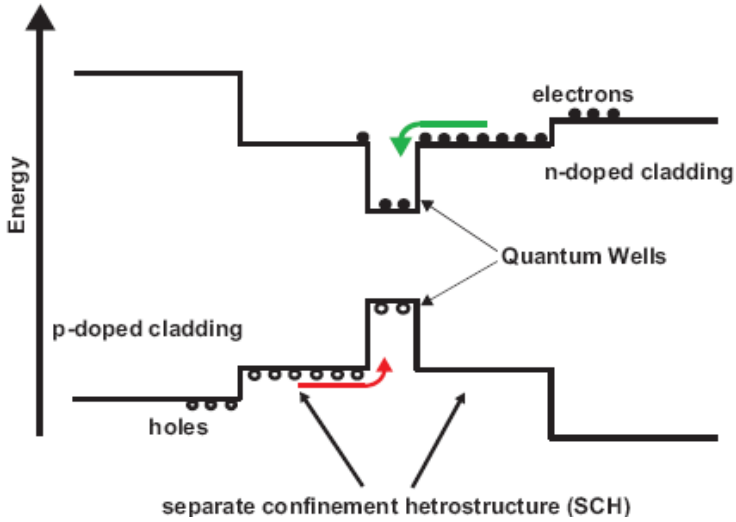

(a) bandgap as a function of distance

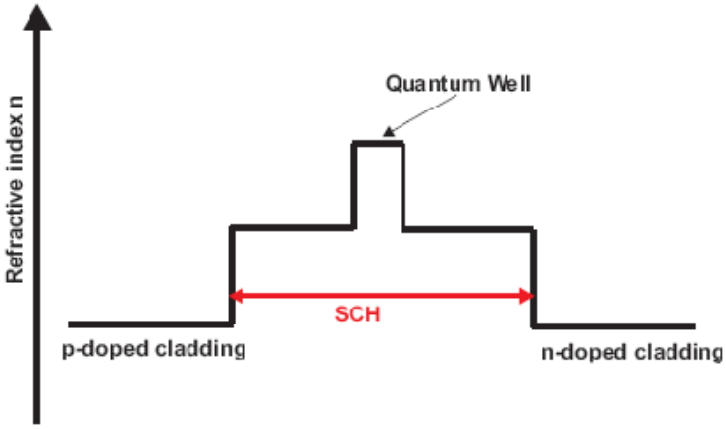

(b) corresponding refractive index profile

Figure 1.3: Bandgap variation and the corresponding refractive index for a simple SOA structure composed of one quantum well surrounded by an SCH

Even though SOA performance does not compare to fiber amplifier technology, there are some features which are very attractive. Unlike fiber amplifiers, SOAs do not require a separate laser diode and are electrically pumped, which improves electrical-to-optical efficiencies. SOAs can be made extremely compact, with typical sizes being 200µm x 100µm x 10µm, and can be mass produced on a single epitaxially grown wafer; each fabricated SOA comes down to only dollars a piece. Being semiconductor-based, SOAs have potential for easy integration within other

semiconductor devices, facilitating on-chip optical routing and computing. Most importantly, the flexibility and tunability of III-V semiconductors means that a single SOA design can be engineered and fabricated to operate at one of the continuum of wavelengths. It is worth noting that the devices we are interested in are monolithic; in other words, they are fabricated on a single epitaxial structure, and the process consists of the standard lithography and deposition only.

Because of these advantages, efforts have been made to improve the performance of SOAs so that they might one day replace the more complex, bulkier, expensive, and less efficient amplifier technologies. Dynamic gain saturation is the primary reason for the low output pulse energies that plagued the SOAs. Dynamic gain saturation occurs when the photon density becomes large (which is more likely to happen toward the output end of the amplifier), and we can no longer ignore the effect that stimulated recombination has on carrier density within the intrinsic region. The incoming light depletes the carrier density via stimulated emission, and this reduction effectively caps (saturates) the amplifier gain. This effect is especially strong for amplification of pulses that are much shorter than τ_g, the phenomenological gain relaxation time, as the gain does not have time to recover to the unsaturated state.

The saturation energy due to dynamic gain saturation E_{sat} is defined as the pulse energy at which the gain has dropped off by 1/e. To keep to conventions used in literature, E_{sat} will be used to denote saturation energy due to dynamic gain saturation. Much of the efforts in pushing the performance of SOAs has been in decreasing the effects of dynamic gain saturation, hence increasing E_{sat}. In the remainder of this thesis we will analyze one particular method of increasing E_{sat}, and then investigate other mechanisms of gain saturation that come into play once E_{sat} is increased.

1.4 Slab Coupled Optical Waveguide

As mentioned in the previous section, our initial objective is to decrease the effects of dynamic gain saturation, thus increasing E_{sat}, which is given by [5]

$$E_{sat} = \frac{\hbar\omega A_a}{\Gamma \frac{dg}{dN}} \tag{1.1}$$

where $\hbar\omega$ is the photon energy, A_a is the area of the active region, Γ is the confinement factor, and dg/dN is a material-dependent parameter called the differential gain. Note that for pulses, the frequency is a range of values and the center pulse frequency should be used for ω in calculations.

Clearly little can be done about the photon energy since the wavelength is determined by device application, and the differential gain is primarily material-dependent, so it cannot be altered by the structure of the device. In fact, the confinement factor Γ is often the easiest parameter to vary when designing a structure. Γ describes how much of the optical mode interacts with the active region itself as light propagates throughout the device. If all of the light is confined in the active region, Γ is nearly 1. Saturation energy will be small if the value of Γ is nearly 1 because high photon density quickly saturates the gain. If some of the optical mode resides outside of the active region, the photon density at the active region decreases; as a result of this, the gain experiences a lower number of photons, staving off gain saturation. For example, if a structure can be designed with $\Gamma = 0.1$, then only 10% of the optical mode would reside at the active region, making it 10 times more difficult to saturate the gain.

There have been numerous schemes which increase E_{sat} by decreasing Γ. Perhaps the most straight forward scheme utilizes a 'tapered' or 'flared' waveguide, greatly increasing the width of the active region while keeping all other parameters the same. A diagram of such a structure is displayed in Figure 1.4. The motivation behind the tapering scheme is simple: increasing the width of the active region elongates the mode, decreasing the photon density at any given point. The result is an increased saturation energy E_{sat}. The tapered waveguide approach has been successfully demonstrated in experiments to greatly reduce the effects of dynamic gain saturation [9].

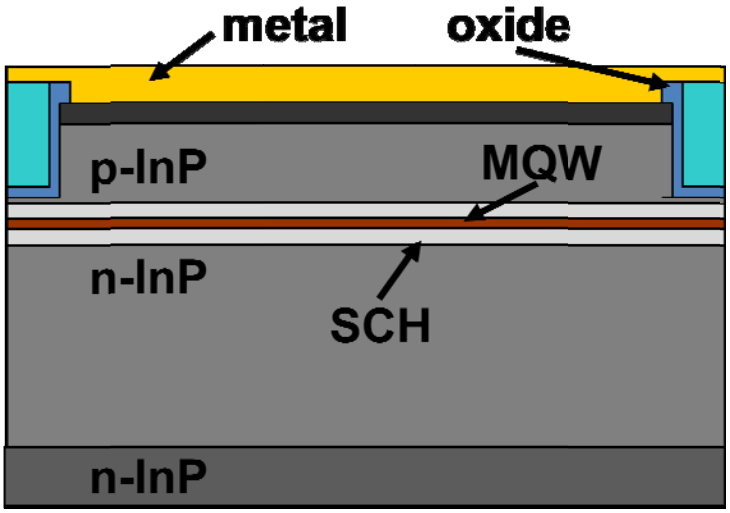

Figure 1.4: An SOA cross-section of a broadened waveguide

While the tapered waveguide approach is successful in increasing E_{sat}, it introduces another problem. The wider waveguide guides and amplifies many higher order modes in addition to the first order transverse mode, which makes these devices nearly unusable for most applications.

Keeping this in mind, we seek a device geometry which increases E_{sat} while still maintaining single-mode behavior. It turns out that at least one such geometry exists: the slab-coupled optical waveguide (SCOW).

The concept of the slab coupled waveguide was conceived in 1973 by E. A. J. Marcatili of Bell Labs, who was working with optical fibers. Marcatili observed that a multimode optical fiber can be made to operate in a single mode regime by coupling it to a slab waveguide [11]. By properly choosing the dimensions of the slab, the higher order modes can be made to radiate away into the slab while the fundamental mode propagates with minimal loss.

This slab-coupled effect is not limited to optical fiber and dielectric slabs. One can easily imagine a similar effect taking place if a smaller (but still multimoded) strip waveguide is coupled to a larger slab. This geometry can be fabricated by appropriate etching of (and deposition on) an epitaxial stack of semiconductors. This allows us to create a monolithic slab-coupled structure in which the slab is a transparent piece of semiconductor, while the ridge is an active region which can provide gain. A cross-section of a potential device is shown in Figure 1.5. Note that the ridge contains the gain region in the form of multiple quantum wells (MQWs) and the slab is composed of InGaAsP. A specific practice device structure will be described in detail in the chapter on our experimental work.

Choosing the appropriate dimensions for the structure in Figure 1.5 allows for an SOA in which only the fundamental optical mode is guided and amplified, yet only a small portion of the mode resides in the gain region, decreasing the confinement factor. For a structure such as this, confinement factors can reach values of 0.01 and below, greatly raising the value for E_{sat}.

The uncommonly large optical mode provides at least one other advantage over conventional SOAs: the mode can be made to be on the order of a fiber optical mode, allowing for fiber-based coupling without the use of complicated optical setups.

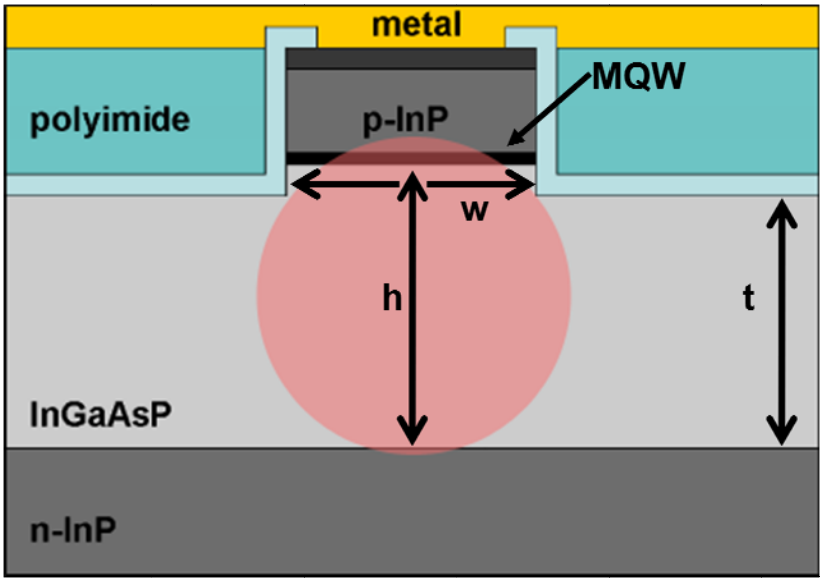

Figure 1.5: A cross-section of proposed slab coupled optical waveguide structure.

The first significant experimental work using SCOW structures for SOAs and semiconductor lasers was, to the author's knowledge, done by Paul Juodawlkis's research group at MIT's Lincoln Laboratory. Using the SCOW concept, output powers of over 1 watt of continuous-wave (CW) light at 1550nm were demonstrated for an SOA -an order of magnitude improvement over previous work[12].

The continuous-wave amplification demonstrated by Lincoln Lab established the SCOWA technology as a viable method of high-power amplification. The remainder of this thesis focuses on the use of SCOWA structures for traveling-wave amplification of high energy picosecond pulses, and the new challenges that high-intensity ultrashort pulses bring.

CHAPTER 2

THEORY

This chapter outlines the physics governing ultrafast pulse amplification in SOAs and develops a model for SOA behavior. We will develop a model which describes the behavior of pulse propagation through our SOA. To do this, we need to analyze the specific processes that change a pulse as it travels through the device.

2.0.1 Linear Model

We begin by focusing on pulses that are not intense enough to induce any non-linearities and exhibit only linear behavior. We assume that a pulse traveling inside the amplifier can be described by a complex envelope A(z,t), where z is the distance from the input end of the amplifier and t is the reduced time. Specifically, $t = T - z/v_g$ where v_g is the group velocity. Using the reduced time t instead of the actual time T places us in the reference frame of the moving pulse, and slightly simplifies the math that comes ahead as well as simplifies interpretation of the resulting model.

We note that A(z,t) retains phase as well as amplitude information, and is a valid way to represent a traveling pulse as long as the pulse duration is much greater than the period of a single optical cycle. In the near IR region where we wish to operate, a single optical cycle is on the order of a few femtoseconds, so picosecond pulses can easily be modeled using this approach.

The envelope A(z,t) must be normalized such that over all time it integrates to the total pulse energy.

$$\int_{-\infty}^{\infty} |A(z,t)|^2 \, dt \tag{2.1}$$

We assume that the gain in the active region depends linearly on carrier density, and that the carrier relaxation time τ_g, which is on the order of a nanosecond, is much greater than the pulse duration. Under these conditions, we can write the time dependent gain as [1]

$$g(z,t) = g_0 \exp\left(-\frac{\int_{-\infty}^{t} |A(z,t')|^2 \, dt'}{E_{sat}}\right) \tag{2.2}$$

where E_{sat} is, as before, the saturation energy due to dynamic gain saturation, and can be written as

$$E_{sat} = \frac{\hbar\omega A_a}{\Gamma \frac{dg}{dN}} \tag{2.3}$$

where A_a is the cross-sectional area of the active region, Γ is the confinement factor, $\frac{dg}{dN}$ is the differential gain, and ω is the center frequency of the pulse.

Note that for pulse energies way below the dynamic gain saturation energy, $\int_{-\infty}^{t} \left|A(z,t')\right|^2 dt' \ll E_{sat}$, so $g(z,t) \cong g_0$.

Ignoring nonlinearities for the time being, we can write the equation governing pulse propagation in the SOA as

$$\frac{\partial A(z,t)}{\partial z} = -i\frac{\beta_2}{2}\frac{\partial^2 A(z,t)}{\partial t^2} + \frac{\Gamma}{2} g(z,t)(1 - i\alpha)A(z,t) - \frac{l}{2}A(z,t) \tag{2.4}$$

We will refer to equation (2.4) as the linear pulse propagation equation. In the linear equation, β_2 is known as the modal dispersion or group-velocity dispersion (GVD) parameter, l describes the waveguide linear loss, and α is the linewidth enhancement factor, which describes changes in material refractive index which accompany changes in the material gain. The fact that the gain the phase of the pulse in addition to the amplitude should come as little surprise; in fact, in any physical

system the real and imaginary parts of the response are related by a principle known as the Kramers-Kronig relation.

Using the normalization equation $\int_{-\infty}^{\infty}|A(z,t)|^2\,dt = E(z)$, we can extract an equation for pulse energy *E(z)* assuming only linear interactions:

$$\frac{dE(z)}{dz} = \Gamma g_0 E_{sat}\left[1 - \exp\left(\frac{E(z)}{E_{sat}}\right)\right] - lE(z) \tag{2.5}$$

2.0.2 Proposed Model

After developing a pulse energy evolution equation for linear interactions only, we wish to include some nonlinearities. We will focus on pulses that are intense enough to induce $\chi^{(3)}$ nonlinearities, but not any higher order nonlinearities.

Remember that most SOAs are made from many materials with varying band gaps. Most of these band gaps, even those larger than the single photon absorption energy, are still below than the two-photon absorption energy, meaning that two-photon absorption (TPA) can happen anywhere in a typical SOA structure. This is shown in a simplified band diagram of the structure in Figure 2.1.

We can incorporate the two-photon absorption effects into our pulse propagation model as

$$\frac{\partial A(z,t)}{\partial z} = -i\frac{\beta_2}{2}\frac{\partial^2 A(z,t)}{\partial t^2} + \frac{\Gamma}{2}g(z,t)(1-i\alpha)A(z,t) - \frac{l}{2}A(z,t) + \frac{(ik_0 n_2 - \beta/2)}{A_{mode}}|A(z,t)|^2 A(z,t) \tag{2.6}$$

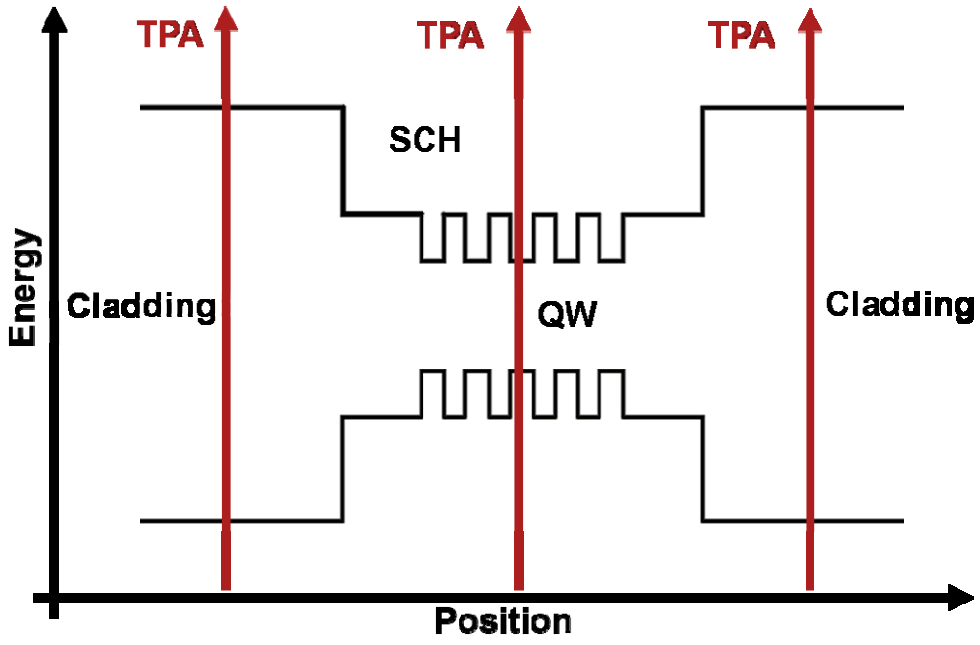

Figure 2.1: TPA can happen anywhere in the structure.

The only change from the linear model of the previous section is the $|A(z,t)|^2A(z,t)$ term, which accounts for the $\chi^{(3)}$ interactions. In this term, k_0 is the free-space propagation vector at the pulse center frequency ω_0, n_2 is the material intensity dependent refractive index, β is the two-photon absorption coefficient, and A_{mode} is a statement describing the cross-sectional mode area in the device. Note that our refractive index n has now been broken up into two parts, a part due to linear interactions n_1, and another due to nonlinear ones, such that $n = n_1 + n_2|A|^2$. A_{mode} can be analytically expressed as

$$A_{mode} = \frac{(\iint |\phi(x,y)|^2 \, dx \, dy)^2}{\iint |\phi(x,y)|^4 \, dx \, dy} \tag{2.7}$$

where $\phi(x, y)$ is the cross-sectional area of the fundamental transverse optical mode.

We noted earlier a change in the pulse amplitude due to gain was accompanied by a change of the phase, a statement that we attributed to a common physical effect described by the Kramers-Kronig relation. Here again we see the same principle: a change in the loss due to TPA is accompanied by a change in the refractive index.

The pulse propagation equation is sometimes referred to in literature as the generalized nonlinear Schrodinger equation, though only because of mathematical similarities and not any physical reason.

Our propagation equation is a nonlinear partial differential equation, and no analytical methods are known for obtaining its solution. A plethora of numerical methods exist for solving this equation, the most widely-used one being the pseudo-spectral algorithm known as the Split-Step Fourier Method. The Split-Step Fourier Method obtains solutions for A(z,t) by assuming that over a small distance *dz* the dispersive and nonlinear effects can be viewed as acting independently. The method then carries out the propagation from *z* to *z*+*dz* in two steps, in which the nonlinearity gets applied independently, and then the dispersion gets applied. A further discussion of the Split-Step Fourier Method is unnecessary as the method is not used in this work, but it can be found in most books on nonlinear optics, for example in [1].

While we cannot solve for A(z,t) analytically, we can, as in the previous section, utilize the $\int_{-\infty}^{\infty}|A(z,t)|^2\,dt = E(z)$ relation to obtain a differential equation for the pulse energy E(z):

$$\frac{dE(z)}{dz} = \Gamma g_0 E_{sat}\left[1 - \exp\left(\frac{E(z)}{E_{sat}}\right)\right] - lE(z) - \gamma(z)E^2(z) \qquad (2.8)$$

$\gamma(z)$ describes the non-linear loss due to two-photon absorption, and is defined as

$$\gamma(z) = \frac{\beta}{A_{mode}} \frac{\int |A(z,t)|^4 \, dt}{(\int |A(z,t)|^2 dt)^2} \tag{2.9}$$

For a pulse with a Gaussian intensity profile and a full-width at half maximum (FWHM) pulse width τ, we can approximate γ by

$$\gamma(z) \approx \frac{\beta}{1.5 A_{mode} \tau} \tag{2.10}$$

Due to dispersion within the device as well as various saturation and loss effects, the pulse width and shape does not necessarily remain constant as the pulse propagates [10][7]. In fact, our simulations as well as experimental measurements suggest that it is typical for the pulse width t to increase by a factor of 2-4 for SCOW amplifiers. Despite this, equation 2.11 remains approximately valid (within approximately 5%) if the τ used is assumed to be the average value of the actual pulse width within the device.

In light of equation 2.9, we can define a new pulse saturation energy E_{TPA}, which is the pulse energy for which SOA gain saturates by 3dB due to two-photon absorption instead of dynamic gain saturation. Using the approximation which yielded eqn. 2.11, we can define E_{TPA} as

$$E_{TPA} = \frac{\Gamma g_0}{e\gamma} \approx \frac{1.5 \Gamma g_0 \tau A_{mode}}{e\gamma} \tag{2.11}$$

Incorporating TPA into our pulse energy evolution model yields not one but two parameters which quantify gain saturation in an SOA: E_{sat} and E_{TPA}. If $E_{sat} << E_{TPA}$, then dynamic gain saturation will saturate the SOA for large pulse energies, and two-photon absorption is not likely to have a significant effect. On the other hand, if $E_{sat} >> E_{TPA}$, then our SOA will saturate due to TPA, and dynamic gain saturation will not

come into play. If the two saturation energies are of the same order, then both mechanisms play a role in saturating the gain.

Our pulse energy evolution equation 2.9, along with the definitions of E_{sat} and E_{TPA} are the most important results of this chapter.

2.0.3 Limitations Imposed by TPA

In this section we will plug in some numbers into the equations developed in the last section to build an intuitive understanding of pulse energy evolution in SOAs.

SOA waveguides with smaller values of modal gain per unit length are more likely to be saturated by two-photon absorption. Most III-V semiconductors can exhibit material gain values up to about 1800cm^{-1}, so the two primary methods available for increasing E_{TPA} in a device is the confinement factor Γ and the mode area A_{mode}. Unfortunately, increasing ΓA_{mode} is difficult, as an increase in Γ by varying geometry more often than not leads to a decrease in A_{mode}. This is indeed the case for SCOW amplifiers. In fact, whereas the entire idea behind the SCOW geometry was to raise the value of E_{sat}, values of E_{TPA} for SCOWA structures are often similar or even smaller than those for conventional SOAs.

If L is the length of an SOA, we can define the input pulse energy $E_{in} = E(z = 0)$ and output pulse energy $E_{out} = E(z = \text{L})$. Note that for small enough pulse energies neither TPA nor dynamic gain saturation are significant, and the unsaturated SOA gain is

$$\frac{E_{out}}{E_{in}} = e^{(\Gamma g_0 - l)L} \tag{2.12}$$

We present the results of a numerical simulation for which we use parameters that correspond to a high power InGaAsP/InP slab-coupled optical waveguide amplifier similar to [8]. The values used for the various parameters are summarized in Table 2.1.

Table 2.1: Simulation Parameters

L	0.8cm
Γ	0.003
l	$0.7cm^{-1}$
E_{sat}	100pJ
A_{mode}	$14\mu m^2$
β	35cm/GW

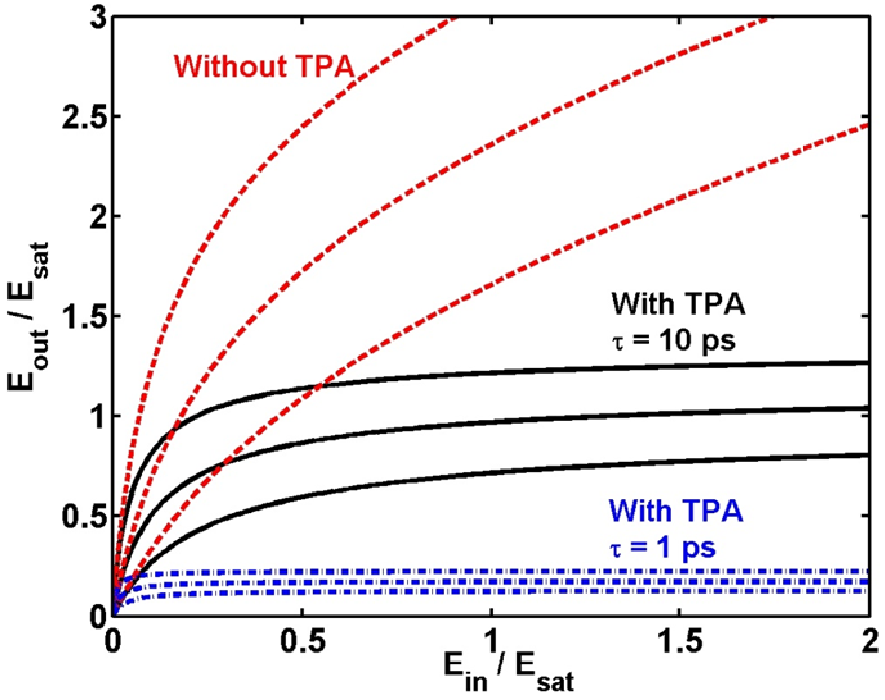

Figure 2.2: E_{out} vs E_{in} curves in the absence of TPA, and in the presence of TPA with pulse widths of 10ps and 1ps.

The value of β was chosen as a reasonable estimate of the actual TPA coefficient which, in III-V semiconductors such as GaAs and InP is typically in the 25-40cm/GW range and varies only slightly with wavelength [3][2].

Figure 2.2 shows E_{out} vs E_{in} curves in the absence of TPA, and in the presence of TPA with pulse widths of 10ps and 1ps. For each case, the three curves correspond to three values of unsaturated material gain g_0: 800cm^{-1} , 1200cm^{-1}, and 1600cm^{-1} . Notice how decreasing the pulse width radically increases effects of saturation due to two-photon absorption for high pulse energies.

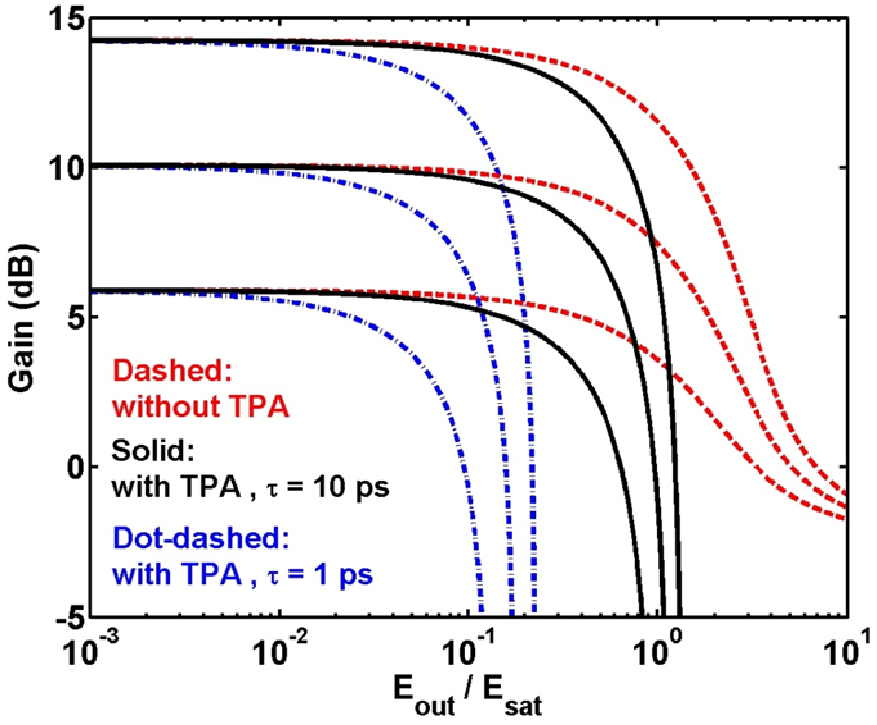

Figure 2.3: Amplifier Gain (in dB) vs. E_{out} curves in the absence of TPA, and in the presence of TPA with pulse width of 10ps and 1ps

The same information is presented in a familiar Gain (in dB) vs E_{out} plot in Figure 2.3. In the absence of TPA, the amplifier gain saturates when E_{out} nears E_{sat}.

However, when TPA becomes significant, amplifier gain caps at a much lower output pulse energy.

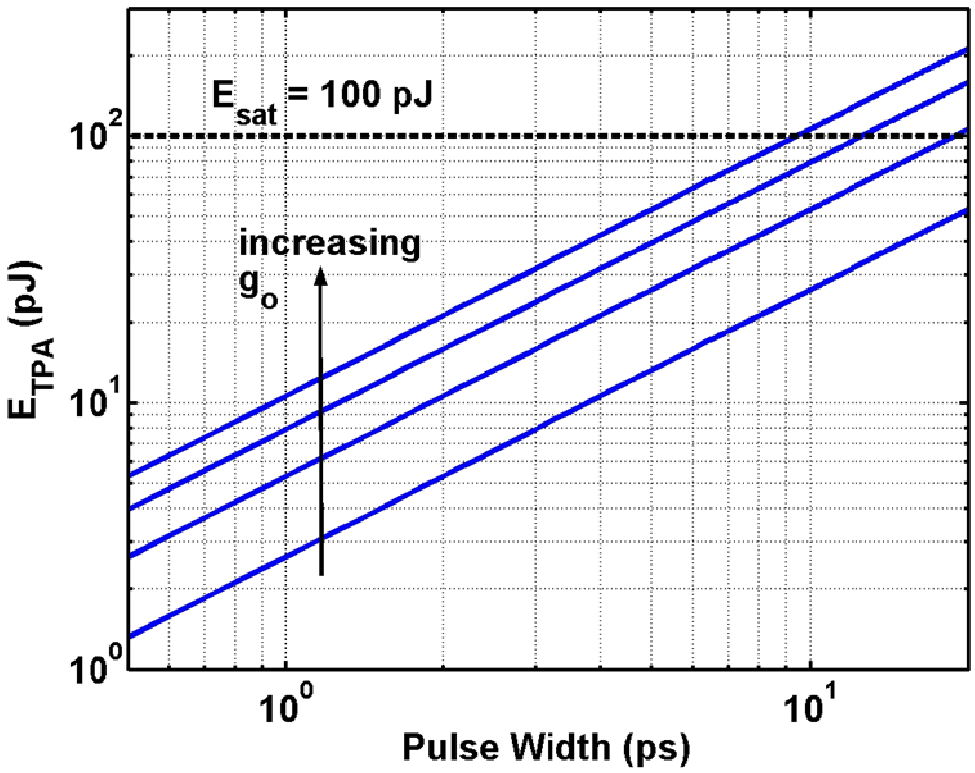

Figure 2.4: E_{TPA} as a function of pulse width τ for various values of unsaturated material gain g_0

We plotted the value of E_{TPA} as a function of pulse width τ for various values of unsaturated material gain g_0 in Figure 2.4. Notice how for longer pulse widths (in this case, longer than 10ps), $E_{TPA} > E_{sat}$, and so the primary mechanism for gain saturation is dynamic gain saturation. However for shorter pulse widths, $E_{TPA} < E_{sat}$, and the limiting mechanism becomes two-photon absorption.

2.0.4 Overcoming TPA

The question then remains: what do we do to get the maximum performance out of our amplifiers? Though it is probably possible to modify the structure slightly by changing the various dimensions to try to match up E_{sat} and E_{TPA} for a given pulse width, we can probably at best get a factor of 2 increase in the output energy, which is not particularly inspiring. There are always other ways, including widening the waveguide, thereby increasing A_{mode}, but then we lose single-moded behavior of SCOWA devices.

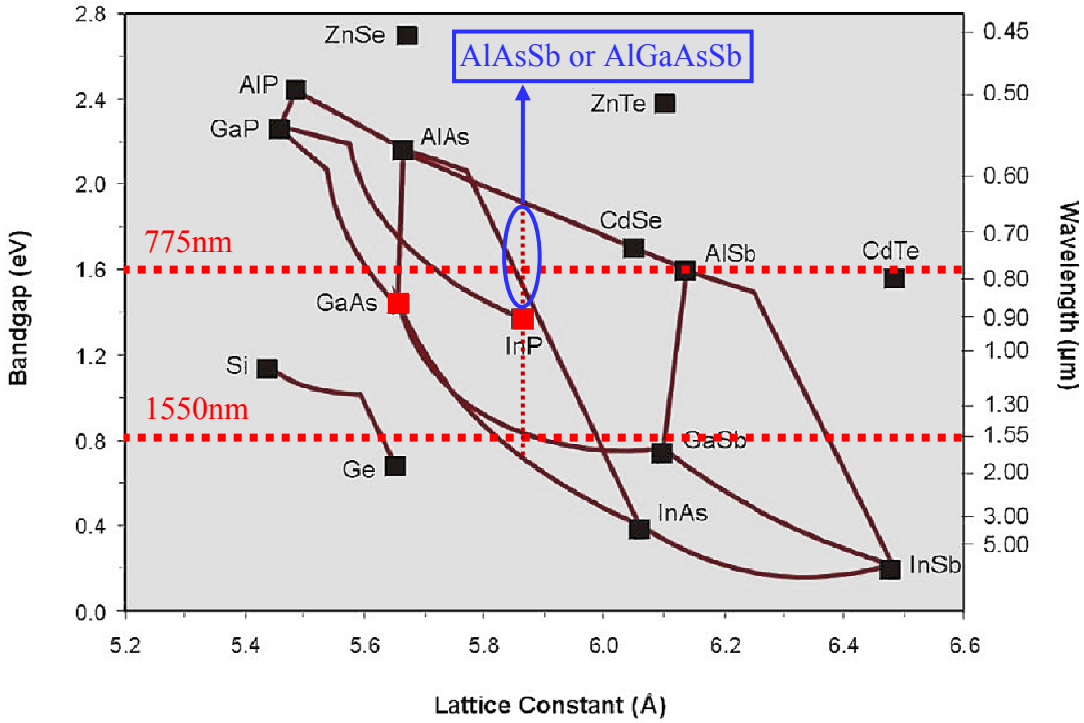

Figure 2.5: Semiconductor reference chart. Note the materials that are lattice-matched to InP and sit above the bandgap which is twice the energy of a 1550 nm photon.

It seems that to make devices that can truly amplify pulses that are both very energetic and very short in time, we need a new approach to avoid TPA altogether.

While the task of developing these new approaches lies with whoever wishes to continue this project, we can at least make one suggestion which could solve the TPA saturation problem.

Remembering that we are working with InGaAsP quantum wells on an InP substrate, we wish to find a material for the slab which avoids TPA. Remember that with the small confinement factors of SCOW devices (0.01 and smaller), the vast majority of the optical mode sits in the slab, so getting rid of TPA in this region virtually removes TPA from the equation. Does such a material exist? It appears that it does. A slightly modified semiconductor reference chart is displayed in Figure 2.5. Note that there are at least two types of materials that are still lattice matched to InP, yet have band gaps that are more than twice the energy of a 1550 nm photon. These materials are AlAsSb or GaAlAsSb, both Antimonides. An added bonus of these materials is that they have an indirect bandgap, making absorption even less likely.

CHAPTER 3

EXPERIMENTAL WORK

In this section we present experimental results to verify the model outlined in the previous chapter. Slab-coupled optical waveguide amplifiers were fabricated and tested, and the results were compared with the model proposed in Chapter 2.

3.0.1 Our Device

The SCOW structures that we used in our experiments were designed at Cornell and fabricated at the Cornell NanoScale Science and Technology Facility with several steps performed at the University of Illinois (UC) Micro/Nanofabrication facility. The specific steps and recipes were outlined and reported in the 2008 PhD thesis of Dr. Faisal Ahmad (who single-handedly designed and fabricated the devices), and therefore will not be repeated here. In this section we will simply outline the basic fabrication steps, and then focus on the final device geometry.

As mentioned earlier, the device structure that we are looking for utilizes Marcatili's slab-coupled optical waveguide concept to decrease E_{sat} by coupling a multiple quantum well (MQW) gain region to a large transparent slab waveguide.

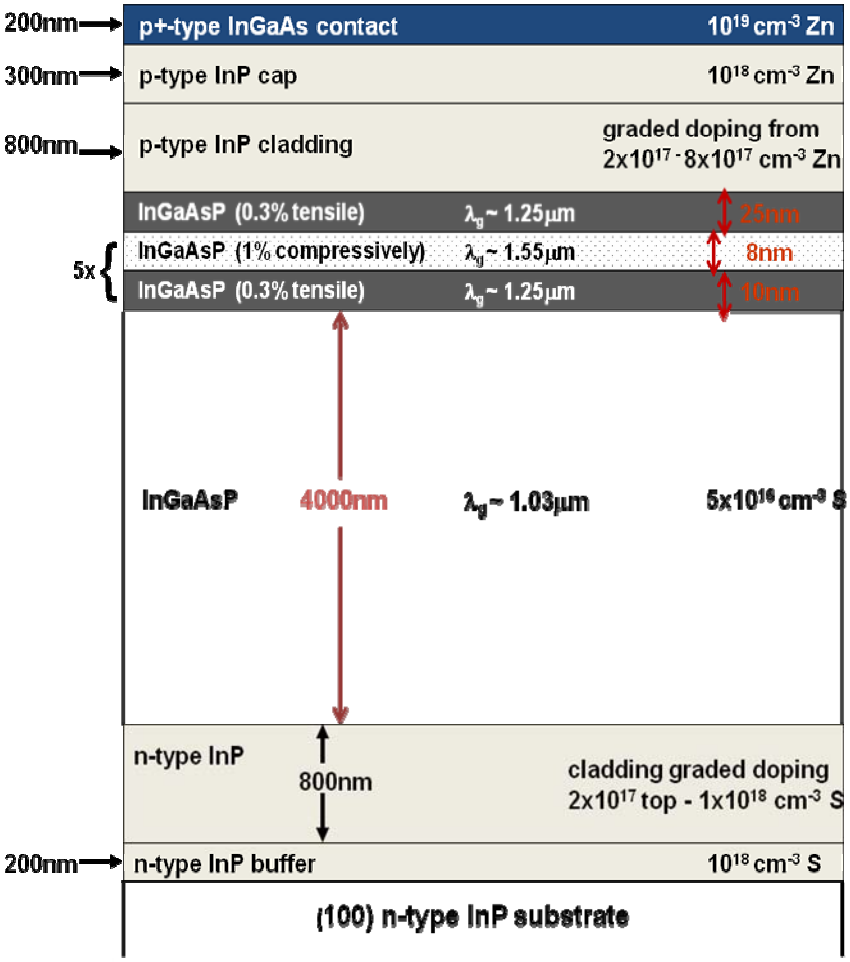

Figure 3.1: Epitaxial Structure

The complete epitaxial structure from which the SCOW devices were fabricated is shown in Figure 3.1. The epitaxial stack was grown by metalorganic chemical vapor deposition (MOCVD) on a Sulfur-doped n-type InP substrate by IQE Ltd. The mode-guiding layer was a lightly-doped (6.5×10^{16} cm^{-3}) 4μm $In_{0.9}Ga_{0.1}As_{0.21}P_{0.79}$ slab with a photoluminescence of 1.03μm. This was followed by a 115 nm active region which consisted of 5 periods of undoped quantum wells and barriers. The 8 nm thick, compressively strained $In_{0.76}Ga_{0.24}As_{0.82}P_{0.18}$ quantum wells had a band gap of 1.55μm, and the 10 nm thick, tensile strained $In_{0.7}Ga_{0.3}As_{0.57}P_{0.33}$ barriers had a band

gap of 1.25µm. The quantum barriers also serve as the secondary confinement heterostructure (SCH). The active region was followed by a 1.1µm Zn(p)-doped InP cladding region, followed by a heavily p-doped InGaAs contact layer

It is important to note here that the band gap for both the barriers and the slab are larger than the single-photon energy at 1550nm, so they are transparent in the linear regime. However, the band gap for both is less than the two-photon energy, so TPA can happen both in the barriers and in the slab.

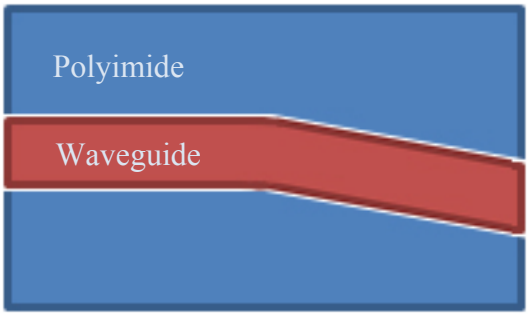

Figure 3.2: SOA Top View. Note the 7˚ tilt to prevent back-reflections.

The fabrication procedure includes lithography, etching, oxide opening, planarization, and finally metallization and the creation of ohmic contacts. The gain region ridge was fabricated to be 4.5µm wide. As mentioned before, all of the specifics can be found in the 2008 PhD thesis of Dr. Faisal Ahmad.

After fabrication, the device facets are created by cleaving along crystal planes which lie perpendicular to the fabricated waveguides. We cleaved the devices to be approximately 6.5 mm in length. The facets possess a natural fresnel reflectance of approximately 30%, and will display fabry-perot behavior if used as amplifiers. To negate the fabry-perot effect, we performed two steps. The first step was the coating of both sides with an anti-reflective (AR) coating consisting of approximately $\lambda/4n$ two materials SiO_2 and Al_2O_3, reducing the facet reflectivity to approximately 1%. The

second step was actually taken in the initial development of the mask: when the devices were designed, they were designed with a tilt so that the output end was actually at a 7˚ angle to the crystal plane and, hence, to the facet. This ensures that any lasing or fabry-perot behavior cannot happen in these devices, as any reflected light would not travel back in the direction of the waveguide. This is demonstrated in Figure 3.2.

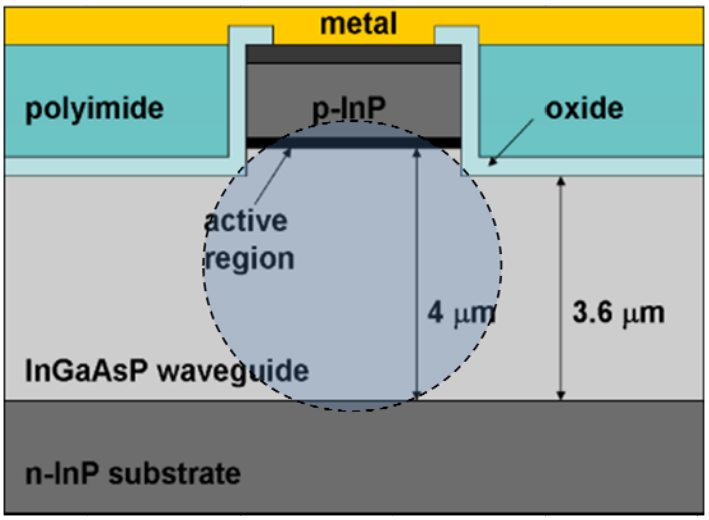

Figure 3.3: Cross-sectional design of our SCOW structure

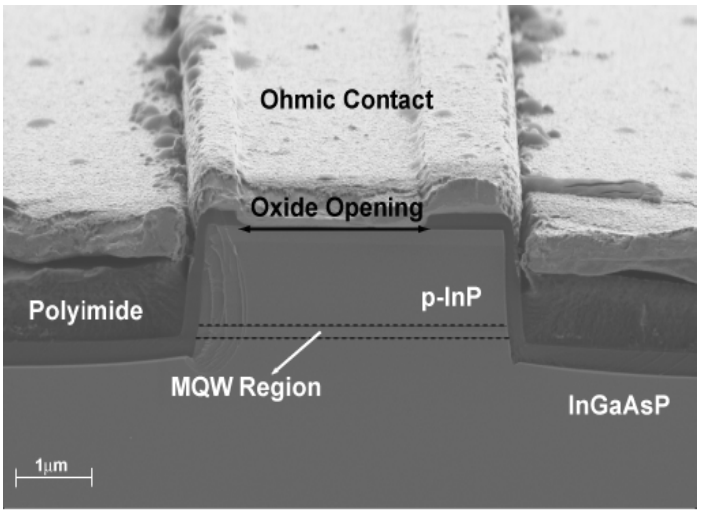

Figure 3.4: Cross-sectional SEM of our SCOW structure

A final schematic of the cross-section of the device is displayed in Figure 3.3, while an SEM of the cross-section is shown in Figure 3.4.

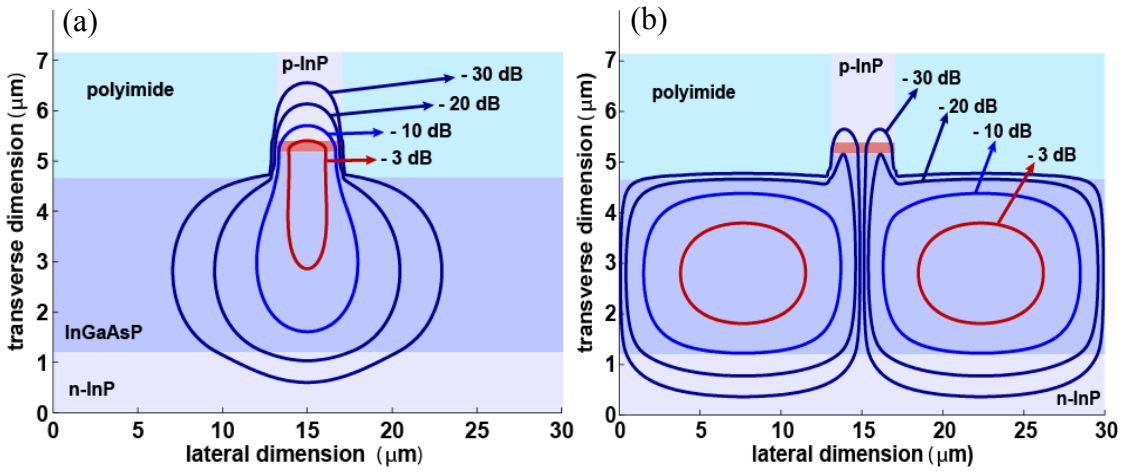

Figure 3.5: (a) Simulation of the fundamental transverse optical mode and (b) the 2nd order transverse optical mode

In section 1.4 of this thesis, the SCOW concept was advertised to exhibit a large modal area with small overlap with the gain region. We used a full vectorial modesolver to confirm this behavior in our structure. Figure 3.5 displays the calculated fundamental and second order mode in our SCOW structure. Notice that the fundamental mode overlaps significantly with the gain region, seeing gain, while the second order mode (along with the higher order modes which are not displayed) sees much less gain. This ensures single-moded behavior in our SOA. The confinement factor for the fundamental mode was calculated to be 0.012.

3.0.2 Experimental Setup

The 6.5mm SCOW amplifiers described in the last section were mounted on a gold-plated copper chuck using indium solder. Indium solder was chosen both as an adhesive, and because it displays high thermal and electrical conductivity. The amplifiers were forward biased using a pair of 3 mil Be/CU dc probe tips. The current

source was an ILX Lightwave Laser Diode Controller module capable of injecting up to 1 A of current.

Because to the length of our devices and the low optical confinement factor, high amounts of current (up to 1A) were needed to bias our amplifiers. This results, by way of joule heating, into a large amount of heat dissipation which became perhaps the most difficult experimental problem to overcome. The chuck on which the amplifiers were mounted was fastened to a gold-plated copper plate, the temperature of which was continuously monitored using a thermocouple. The plate was cooled by a thermo-electric Peltier heat pump, which was controlled by an ILX Lightwave temperature controller using the feedback from the plate thermocouple. A much larger Peltier module, with its own thermocouple and temperature controller were mounted slightly below, creating a two-stage temperature controller. The waste heat was fed to a large aluminum heatsink.

The two-stage temperature controller made it possible to maintain the copper chuck at a cool 12˚C even with as much as 1A injected into the devices. However, the relatively low temperature of the chuck created another problem. It turns out that 12˚C is near or below the dew point during non-winter seasons. Therefore, on most non-winter days, water was observed to condense on the chuck and the SOA when it was kept at 12˚C. This condensation affected the electrical properties of on the surface, changing the surface resistance, making the experiment unstable, and even damaging the devices. To reduce the condensation effect, we surrounded our experimental assembly with an acrylic box, and purged the box with dry nitrogen.

The nitrogen-purged acrylic box was successful in dropping the humidity level to a low enough point that condensation on our devices was no longer a problem.

However, the box itself presented yet another experimental nightmare. It turned out that as the heat-sink was also inside the box, the temperatures inside the box would slowly rise over the course of an experiment, and eventually the high ambient temperature would make it impossible for the thermoelectric coolers to maintain constant chuck temperature. We solved this problem by passing the incoming dry nitrogen through a copper coil which was dipped in a vat of liquid nitrogen. Using this method, we were able to bring the ambient temperature of the box itself down to 12-14˚C.

The input optical pulses were produced by a home-built Erbium-doped fiber modelocked laser, which produced picosecond pulses at 30-33MHz. The pulses had a bandwidth of 35 nm centered around 1550 nm and a measured full-width at half maximum (FWHM) temporal width of 2.2 ps. The pulses were amplified using a JDS Uniphase Erbium-doped fiber amplifier (EDFA). The input pulse energy was varied between 5 pJ and 100 pJ using a variable attenuator which consisted of a half-wave plate and a polarizer. The attenuator setup also doubled as an input polarization controller; since our gain region contains quantum wells, only TE polarized light will see gain. The resulting light was split using a 50/50 fiber coupler, with 50% of the light going to an ILX Lightwave integrating sphere power meter, and the other 50% going to the amplifier.

The light was coupled into the amplifier by using a lens fiber mounted on an automated three axis stage. Once the light was coupled, the output was collimated using a 0.68 NA aspheric lens, and the output was sent to a second ILX integrating sphere power meter. On occasion, the light was also diverted from the power meter by mirrors and sent to other instruments, such as a spectrum analyzer and an autocorrelator.

Despite our best efforts to shield the amplifiers from the environment, the experimental setup remained relatively unstable. Specifically, any minor ambient thermal fluctuations would throw the input out of alignment due to thermal expansion.

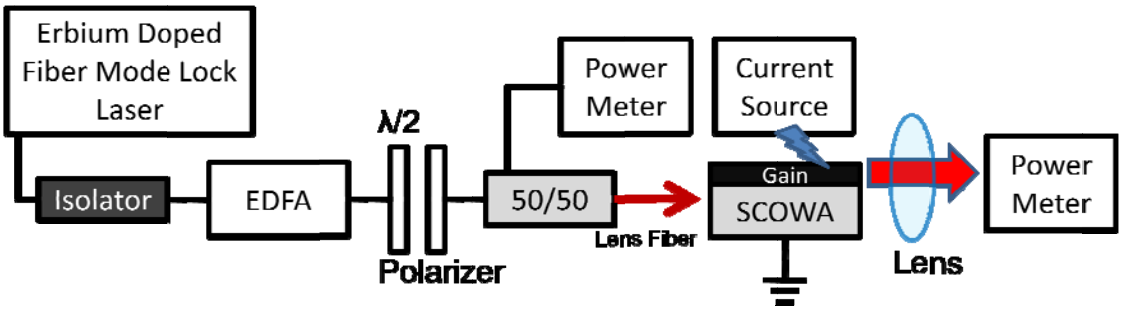

Figure 3.6: A schematic of the experimental setup.

To date we have not been able to produce an experimental setup that remains perfectly steady for more than approximately 10 minutes, so every data-taking run was done as fast as possible. To facilitate this, data from both power meters was simultaneously logged using a Matlab-based GPIB acquisition program.

The basic experimental setup is summarized in Figure 3.6.

3.0.3 Data and Analysis

The basic data taken from the experiment described in the previous section is shown in Figure 3.7. The figure shows the output vs input pulse energies for bias currents of 500mA, 750mA, and 1000mA. Note that transparency was observed somewhere between 300mA and 400mA and the frequency spectrum at the output appeared by be unchanged from the input spectrum.

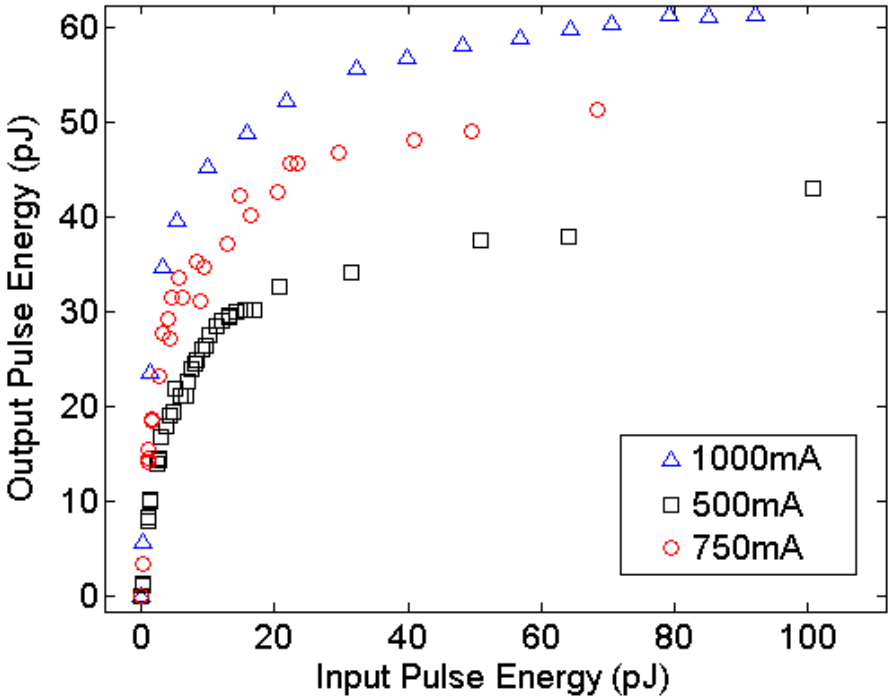

Figure 3.7: Experimental Data

The steep slope at the lowest pulse energies represents the unsaturated gain, whereas the slope at the large pulse energies represented the saturated gain. The goal was to use this data to verify which of the two models (the original linear model, or the proposed TPA model) actually describes pulse energy evolution in our SOAs. The flattened slope for higher pulse energies seems to suggest that not only is the material gain saturating, but another mechanism is causing drastic amounts of loss in the device.

We first attempted to fit the original linear model to our data, and the results are displayed in Figure 3.8. Although we were able to match up the model for lower pulse energies, no sensible selection of parameters could make the model fit at the higher energies. We therefore conclude that, as we anticipated in the theory section, the linear loss model fails for high energy pulses.

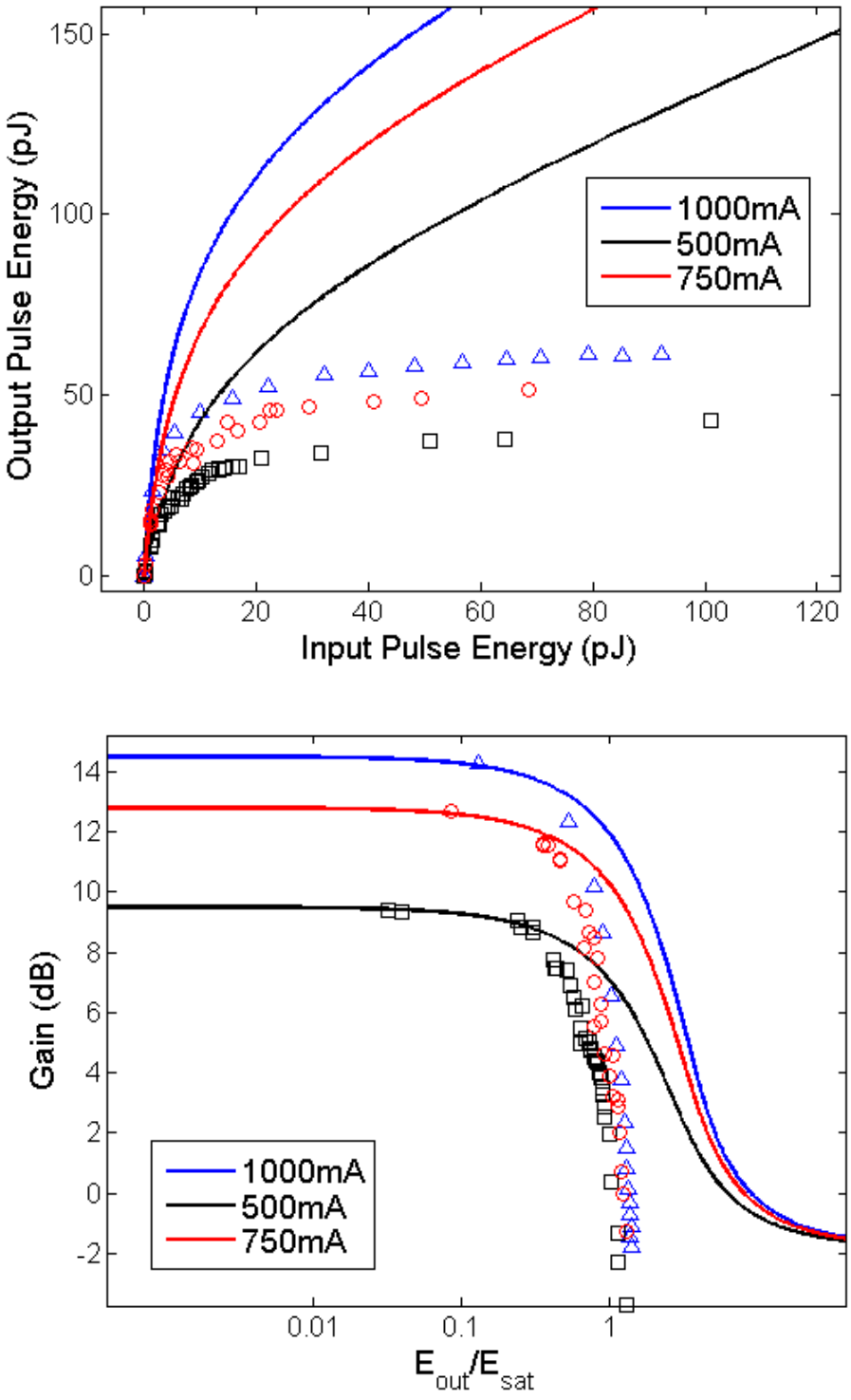

Figure 3.8: Linear model fits to experimental data

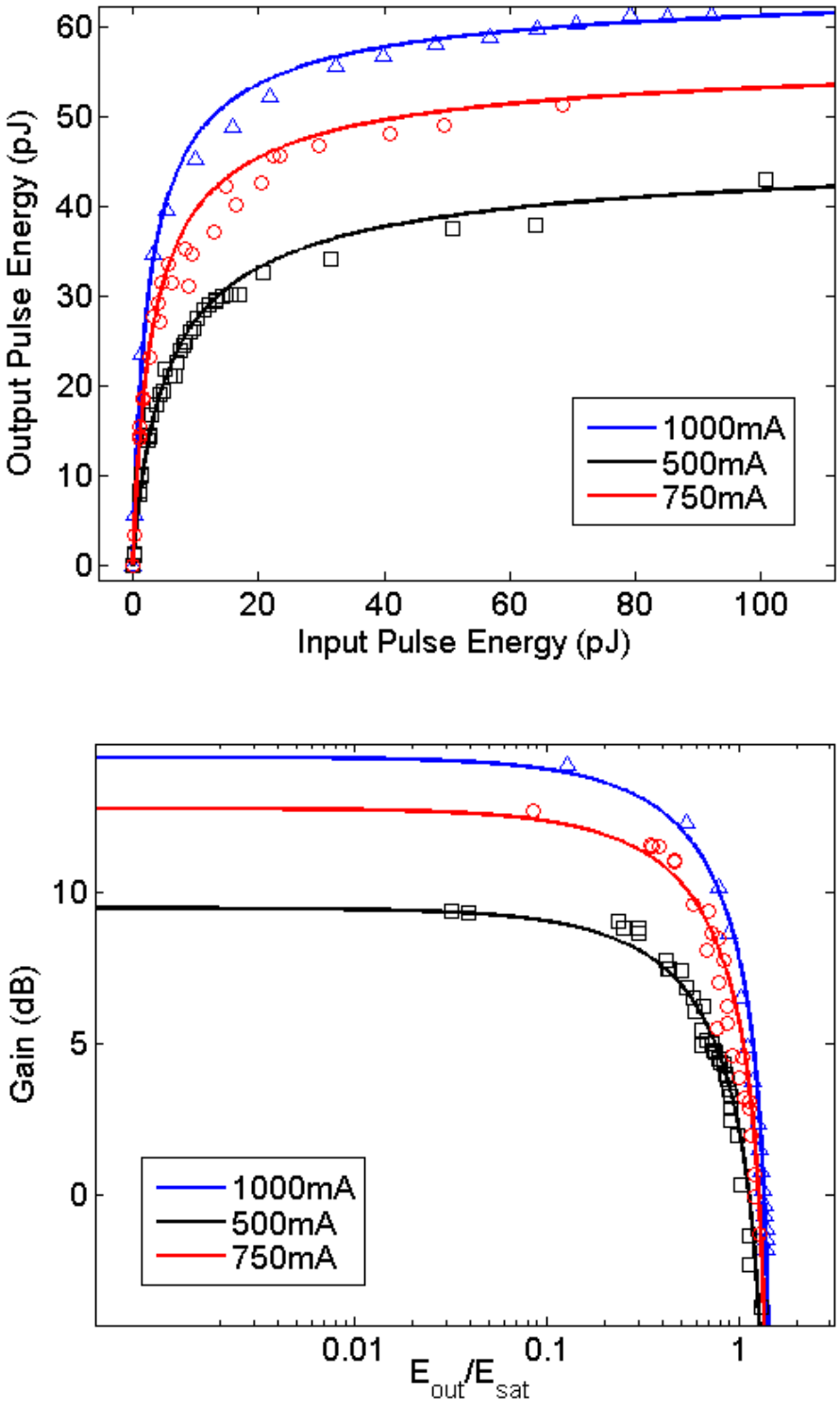

Figure 3.9: Proposed model fits to experimental data

In Figure 3.9, we display our fit of the proposed model which incorporates TPA to our data. We observe that this model fits very well for both low and high pulse energies. The excellent fits confirm that TPA is indeed a substantial saturation mechanism in our devices, and that our proposed model accurately describes SOA behavior when both TPA and dynamic gain saturation are present.

CHAPTER 4

CONNECTION TO MODELOCKED LASERS

The final topic of discussion in this thesis is the application of the new ideas that we have learned to SCOW semiconductor modelocked lasers (SCOWLs). As we mentioned in the first chapter of this thesis, SOAs and semiconductor lasers are intricately linked. In fact, the only real difference is that in an SOA the feedback is suppressed via anti-reflective (AR) coatings and other methods, whereas in a laser the feedback is typically modified via high-reflective (HR) and AR coatings to obtain optimal laser performance.

In this section we verify that the TPA saturation effect that we have quantified in the earlier chapters places a direct limitation on the performance of semiconductor modelocked lasers. Our proposed model clearly shows the tradeoff between potential SOA output pulse energies and the pulse width. It is clear that to obtain larger output pulse energies for a given device, we must reduce the effects of TPA by increasing the pulse width. Since we build SOAs and semiconductor lasers in the same way, we expect this tradeoff to apply to high power semiconductor modelocked lasers.

We will not dwell on analytical arguments in this chapter, but instead demonstrate our supposed tradeoff experimentally. We used the same SCOW structure described in section 3.1 to make semiconductor modelocked lasers. The design and characterization of these devices was the topic of Dr. Faisal Ahmad's 2008 PhD thesis, so we will not spend much time on describing these devices. The device was 9 mm long with one facet AR coated, while the other facet was HR coated. The cavity incorporated a gain section as described earlier in this thesis and a reverse-biased saturable absorber section to facilitate passive modelocking.

The gain region of the device was forward-biased at 800 mA, 1200 mA, and 1600 mA, whereas the saturable absorber region was reverse-biased at 1.5 V ¬3 V. For these values, the SCOWL modelocked at 4.62 GHz, the expected frequency given the device length. Tuning the reverse-bias voltage affected the pulse width via various mechanisms. For example, an increase in reverse bias results in faster saturable absorber relaxation, and also changes the loss saturation energy. Both of these effects change the pulse energy, changing how much the gain saturates, etc.

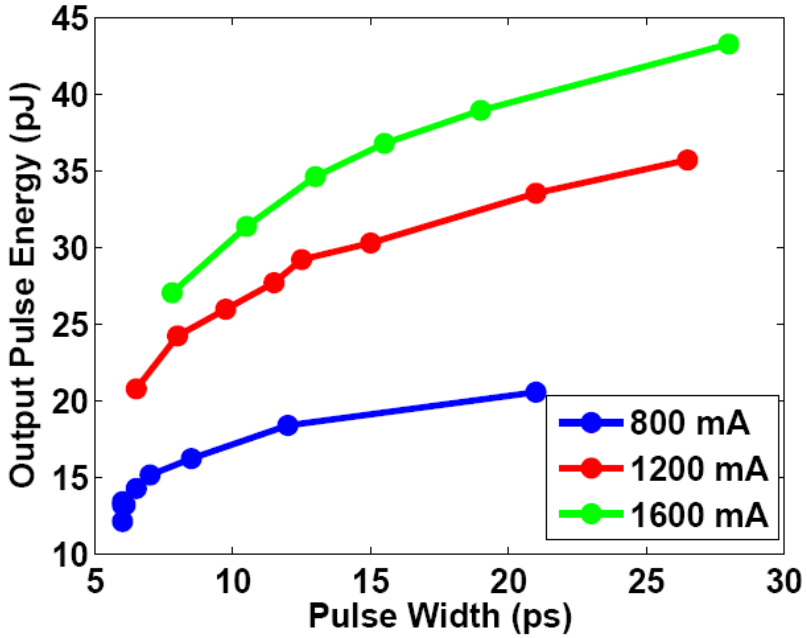

Figure 4.1: Pulse energy vs Pulse width for SCOWL device at various currents.

Figure 4.1 displays the output pulse energy as a function of the pulse width for the three forward-bias currents. The plot was made by varying the reverse-bias voltage. The data indicates a direct correlation between pulse width and output pulse energy. This correlation is consistent with our model assumptions, and it‘s plausible that gain saturation due to TPA can explain some of the positive trend in this curve.

CHAPTER 5

CONCLUSION

In this thesis we studied pulse energy evolution within Slab-Coupled Optical Waveguide Amplifiers which is a subclass of semiconductor optical amplifier capable of amplifying high power picosecond pulses. We presented a new pulse energy evolution model that incorporates the effects of gain saturation due to two-photon absorption, and verified the model by performing experimental calculations and extracting material parameters based on our home-built InGaAsP/InP SCOWA devices.

The results of this thesis have a profound effect on high-energy ultrashort pulse amplification. Only when the saturation energy due to dynamic gain saturation is improved in the conventional semiconductor optical amplifiers that we see a new mechanism for energy saturation to take place – two photon absorption. Two photon absorption became the new limiting factor that can and will cap output pulse energies within the InP-based semiconductor optical amplifiers. Furthermore, we showed that the same effect will be a limiting factor in output pulse energies for ultrashort pulse generation using semiconductor modelocked lasers. New strategies are needed for the next generation of semiconductor optical amplifiers and semiconductor modelocked lasers capable of producing high-energy ultrashort pulses. One such strategy, the use of antimonides as a waveguide/slab material, is briefly discussed.

BIBLIOGRAPHY

[1] Govind P. Agrawal. *Nonlinear Fiber Optics, 2nd Ed*. Academic Press, 1995.

[2] R. W. Boyd. *Nonlinear Optics*. Academic Press, 2003.

[3] F. Mollot D. Vignaud, J. F. Lampin. 'Two-photon absorption in InP substrates in the 1.55 um range'. *Applied Physics Letters*, **85**:239–241, (2004).

[4] B.E. Deal and A. S. Grove. 'General Relationship for the Thermal Oxidation of Silicon'. *Journal of Applied Physics*, **36**:3770, (1965).

[5] F. Rana F. R. Ahmad. 'Passively Mode-Locked High Power (210 mW) Semiconductor Lasers at 1.55 um Wavelength'. *IEEE Photonics Technology Letters*, **20**:190–192, (2008).

[6] Y. W. Tseng, F. R. Ahmad, M. A. Kats, F. Rana. 'Energy Limits Imposed by Two-Photon Absorption for Pulse Amplification in High Power Semiconductor Optical Amplifiers'. *Optics Letters*, **33**:1041–1043, (2008).

[7] N. A. Olsson G. P. Agrawal. 'Self-Phase Modulation and Spectral Broadening of Optical Pulses in Semiconductor Laser Amplifiers'. *IEEE Journal of Quantum Electronics*, **25**:2297–2306, (1989).

[8] B. Chann D. J. Ripin R. K. Huang P. W. Juodawlkis J. J. Plant, J. T. Gopinath. '250 mW, 1.5 um monolithic passively mode-locked slab-coupled optical waveguide laser'. *Optics Letters*, **31**:223–225, (2006).

[9] D. Welch L. Goldberg, D. Mehuys. 'High power mode-locked compound laser using a tapered semiconductor amplifier'. *IEEE Photonics Technology Letters*, **6**:1070–1072, (1994).

[10] A. Dienes J. P. Heritage P. J. Delfyett M. Y. Hong, Y. H. Chang. 'Subpicosecond Pulse Amplification in Semiconductor Laser Amplifiers: Theory and Experiment'. *IEEE Journal of Quantum Electronics*, **30**:1122–1131, (1994).

[11] E. A. Marcatili. 'Slab-coupled waveguides'. *Bell System Technology Journal*, **53**:645–672, (1975).

[12] R. K. Huang L. J. Missaggia J. P. Donnelly P. W. Juodawlkis, J. J. Plant. 'High-Power 1.5-um InGaAsP-InP Slab-Coupled Optical Waveguide Amplifier'. *IEEE Photonics Technology Letters*, **17**:279–281, (2005).